

**Article title:**

A systematic procedure to optimise dose and image quality for the measurement of inter-vertebral angles from lateral spinal projections using Cobb and superimposition methods

**Authors:**

Dr Bashar Al Qaroot<sup>a,b</sup>, Prof Peter Hogg<sup>a</sup>, Dr Martin Twiste<sup>a,c</sup>, and Prof David Howard<sup>a,d</sup>

<sup>a</sup>Centre for Health Sciences Research, University of Salford, UK

<sup>b</sup>Prosthetics and Orthotics department, The University of Jordan, Jordan

<sup>c</sup>UNIPOD – United National Institute for Prosthetics & Orthotics Development, University of Salford, UK

<sup>d</sup>School of Computing, Science & Engineering, University of Salford, UK

Dr Bashar Al Qaroot Corresponding author	Prof Peter Hogg	Dr Martin Twiste	Prof David Howard
BSc, MSc, PhD	BSc, MSc	BSc, MSc, PhD	BSc, PhD
Assistant Professor (University of Jordan) Honorary Research Fellow (University of Salford)	Diagnostic Imaging Research Programme Lead	Senior Lecturer	Associate Head (Research) EPS
Office 204 Prosthetics and Orthotics department Faculty of Rehabilitation Sciences University of Jordan, Amman, 11942, Jordan.  T: +962(0)777 151 856 E: b.qaroot@ju.edu.jo	L608 Allerton Building University of Salford Salford, M5 4WT, UK  T: +44(0) 161 295 2492 E: p.hogg@salford.ac.uk	PO53 Brian Blatchford Building University of Salford Salford M5 4WT, UK  T: +44(0) 161 295 7029 E: m.twiste@salford.ac.uk	UG3 Newton Building University of Salford Salford M5 4WT, UK  T: +44(0) 161 295 3584 E: d.howard@salford.ac.uk

**Abstract**

Background: Patients with vertebral column deformations are exposed to high risks associated with ionising radiation exposure. Risks are further increased due to the

serial X-ray images that are needed to measure and assess their spinal deformation using Cobb or superimposition methods. Therefore, optimising such X-ray practice, via reducing dose whilst maintaining image quality, is a necessity.

**Objectives:** With a specific focus on lateral thoraco-lumbar images for Cobb and superimposition measurements, this paper outlines a systematic procedure to the optimisation of X-ray practice.

**Methods:** Optimisation was conducted based on suitable image quality from minimal dose. Image quality was appraised using a visual-analogue-rating-scale, and Monte-Carlo modelling was used for dose estimation. The optimised X-ray practice was identified by imaging healthy normal-weight male adult living human volunteers.

**Results:** The optimised practice consisted of: anode towards the head, broad focus, no OID or grid, 80kVp, 32mAs and 130cm SID.

**Conclusion:** Images of suitable quality for laterally assessing spinal conditions using Cobb or superimposition measurements were produced from an effective dose of 0.05mSv, which is 83% less than the average effective dose used in the UK for lateral thoracic/lumbar exposures. This optimisation procedure can be adopted and used for optimisation of other radiographic techniques.

## **Keywords**

Optimisation of X-ray imaging, lateral thoraco-lumbar imaging, exposure dose reduction, image quality preservation, Cobb method, superimposition method.

## **Introduction**

In X-ray imaging, risks as severe as cancer may be imposed on patients due to

ionising radiation exposure. This is why as low as reasonably achievable (ALARA) dose should always be adopted, but not at the expense of image quality<sup>1, 2</sup>. Optimising X-ray practices is thus essential for imaging people. This is particularly important when performing serial imaging<sup>3-5</sup>.

Serial imaging is often required when treating young patients with vertebral column deformations (thereby imposing high risks such as breast cancer<sup>6</sup>). Imaging is commonly performed using plain X-ray<sup>7, 8</sup> where images are used to monitor and assess a patient's deformation using 'Cobb' or 'superimposition' method for inter-vertebral angle<sup>7</sup> or range of motion<sup>8</sup> measurements, respectively. Optimisation associated with these measurement methods should be based on minimising dose whilst maintaining image quality suitable for taking accurate measurements to assess vertebral deformation.

Several publications<sup>6, 9-14</sup> have outlined how manipulating some acquisition parameters may result in dose reduction whilst maintaining image quality for accurate Cobb method measurements. Some found the postero-anterior (rather than antero-posterior) projection is an effective way of reducing dose to critical organs<sup>9</sup>. Others have demonstrated that dose can be reduced and image quality maintained by manipulating certain acquisition parameters, for instance: not using a secondary radiation grid (or using an air gap technique)<sup>9-12</sup>; increasing both voltage and inherent beam filtration<sup>6, 14</sup>; and using digital imaging equipment<sup>11-13</sup>. However, no publication has considered in a single study outlining the combined effect of the different acquisition parameters. Also, whilst postero-anterior and antero-posterior projections of the spine have been considered within many publications, only some have addressed lateral projections of the spine<sup>15-16</sup>. Furthermore, all publications

have focused on dose reduction for the Cobb method, whereas none have considered the superimposition method.

In an attempt to overcome this gap in the literature, this study has considered the combined effect of the main acquisition parameters (discussed below) within one optimisation procedure in order to identify the acquisition parameters settings that result in adequate image quality from minimal dose. In this study, the lateral thoraco-lumbar spine (9<sup>th</sup> thoracic to 3<sup>rd</sup> lumbar vertebra (T9 to L3)) was selected for imaging because spinal deformations are common in this region<sup>17</sup>.

This study, therefore, aims to outline a systematic procedure to the optimisation of X-ray practice with a specific focus on lateral thoraco-lumbar (T9 to L3) images for Cobb and superimposition measurements.

## **Methodology**

For the purposes of optimisation, image quality was appraised using a bespoke visual analogue rating scale (VARS), and dose was estimated using software PCXMC 2.0.1.3<sup>18</sup> (STUK, Finland).

The VARS' five criteria (given in Table 1) met the requirements for Cobb and superimposition methods, and were informed by the European guidelines on quality criteria for lateral lumbar radiographs<sup>19</sup>. To verify appraisers' consistency in using the VARS, 3 radiographers and 1 orthotist scored 50 lateral thoraco-lumbar images of clear to not clear qualities. These images were chosen, by 2 independent radiographers, from a pool of just under 1000 images acquired at different acquisition parameters. Cohen's Kappa coefficient<sup>20</sup> demonstrated high consistency between the 4 appraisers (as seen in Table 1), and on this basis 1 appraiser scored

all images in this study. Cohen's Kappa coefficient test was used rather than weighted Cohen's Kappa coefficient test because the later is used when the agreement on a specific category(s) within the scale is to be investigated. However, in this study, this was not the case as there was only two categories on the scale (clear or not clear) and they both were equally important<sup>20,21</sup>

Table 1. This gives the agreement level between the 4 appraisers based on Cohen's kappa coefficient results in relation to each of the five criteria that formed the VARS. 'A1', 'A2', 'A3', and 'A4' are appraisers 1, 2, 3, and 4, respectively. Based on Landis and Koch<sup>35</sup>, a Kappa of 0.81 to 1.00 indicates substantial to almost perfect agreement (presented as '•'); and Kappa of 0.61 to 0.80 indicates moderate agreement (presented as 'Θ').

Criteria		Appraiser combinations					
		A1 to A2	A1 to A3	A1 to A4	A2 to A3	A2 to A4	A3 to A4
Visualisation of the...	...superior vertebral endplate	•	•	•	•	•	•
	...inferior vertebral endplate	•	•	•	•	•	•
	...inter-vertebral spaces	Θ	•	•	•	Θ	•
	...pedicles	Θ	•	•	•	•	•
	...spinous processes	•	•	•	•	•	•

Due to time restrictions and the large number of dose measurements that were needed, effective dose (E) was estimated from air Kerma using Monte Carlo simulation<sup>18, 22, 23</sup> with International Committee of Radiology Protection 103 weighting factors<sup>24</sup>.

The optimisation was conducted in 2 parts. Part 1 consisted of an anthropomorphic phantom based investigation into the effect of the main acquisition parameters on image quality and E, and involved a computed radiography (CR) system (Arcoma-Arco-Ceil, 3.5mm total filtration), an AGFA 35-X digitiser (AGFA, Belgium), an NX 3.7.0.0 workstation, and an Alderson-Rando anthropomorphic phantom (Supertech,

USA). Part 2 consisted of healthy male volunteers based imaging validation that took into account the results from part 1. In particular, 9 normal-weight (body mass index of 18.50 to 24.99 kg/m<sup>2</sup>) adult (18-40 year-olds) living human volunteers with heights ranging from 155-200cm were recruited. Each volunteer was imaged 6 images in different positions (i.e. flexion, extension and neutral) as part of another investigation that was held to compare restrictions on spinal mobility (measured using Cobb and superimposition methods) whilst wearing different spinal orthoses. Due to the unrelated focus, the results of this investigation will be published in a separate paper. In this part, a CR MEDIO 50 system (Philips, Netherlands, 3.5mm total filtration), an AGFA 30-X digitiser (AGFA, Belgium), and NX 3.7.0.0 workstation were used. For both studies, the same look-up table was used to display and process the images (see table 2). Also, equipment quality control tests met manufacturer specifications.

Table 2. Look-up table specifications

Criterion	Value
Speed class	400
MUSI contrast	3
Noise reduction	0
Extended window left	-0.2
Extended window right	0.2
Threshold	0.1
Edge contrast	0
Latitude reduction	0
Sesitometric curve	RP1KT
Contrast Nr of levels	3

Ethical approval was granted for the human (part 2) study, whereby each participant consented before taking part in the study. Females were excluded, because they carry higher risks than males due to increased organ radio-sensitivity and maybe an

unknown pregnancy.

### **1) Overview of part 1 (phantom study)**

Investigating the effect of the main acquisition parameters (discussed below) on image quality and E is best performed with a full-factorial investigation that takes into account all possible combinations between the settings across all acquisition parameters. However, such a procedure would be time consuming due to the extensive number of experimental possibilities. Instead, the main acquisition parameters were divided into a primary and secondary set, whereby only the primary set was subject to a full-factorial investigation.

X-ray photon quantity, penetrability and intensity are primarily controlled by kilovolt peak (kVp), milliamp seconds (mAs) and source to image detector distance (SID). These were considered to be the primary acquisition parameters as they directly affect image quality and dose. In turn, anode heel effect, focal spot, object to image receptor [IR] distance (OID), air gap, and grid were considered as the secondary acquisition parameters as they have a lesser effect on image quality and dose than the primary acquisition parameters.

The procedure by which the effect of the main acquisition parameters on image quality and E was investigated consisted of 3 steps:

Step 1 – Establish the factorial set of primary acquisition parameters

Step 2 – Optimise each secondary acquisition parameter individually  
(using a factorial set of primary acquisition parameter combinations,  
whilst the other secondary acquisition parameters are fixed)

Step 3 – Conduct a full-factorial primary acquisition parameter investigation  
(whilst secondary acquisition parameters are fixed at their optimised settings)

During these 3 steps, the phantom was positioned in accordance with Clark<sup>25</sup>. Collimation was limited to T9 to L3 in accordance with the recommendations from the Institute of Physics and Engineering in Medicine<sup>26</sup>.

## **2) Overview of part 2 (human study)**

The results from part 1 were applied within part 2 to identify suitable acquisition parameter settings.

## **3) Details of part 1 (phantom study)**

Step 1 – Establish a factorial set of primary acquisition parameters

For each of the 3 primary acquisition parameters (i.e. kVp, mAs and SID), 10 fairly evenly distributed settings were chosen from their available range of settings. Different combinations between these settings (where each combination involved all 3 primary acquisition parameters) were then used for imaging the phantom, until a combination was identified that produced an image of suitable quality based on the VARS results. Throughout this testing, the secondary acquisition parameters were fixed, based on the European guidelines on quality criteria for lateral lumbar radiographs<sup>19</sup>.

Additional primary acquisition parameter settings were then chosen via a systematic procedure, using 2 settings below and 1 above each of the 3 obtained settings. The reason for choosing only 1 setting above (rather than 2 settings as with below) is



based on the VARS results in that images acquired at 2 settings above were mostly associated with unsuitable image quality. This gave a total of 4 settings for each of the 3 of primary acquisition parameters (i.e. 1 initial setting plus 2 settings below and 1 setting above) and hence a total of 64 combinations ( $4 \text{ kVp} \times 4 \text{ mAs} \times 4 \text{ SID} = 64$ ).

## Step 2 – Optimise each secondary acquisition parameter individually

### *Anode heel effect*

Using the 64 combinations identified in step 1, 64 images were acquired at each: 1) anode towards the head; and 2) anode towards the feet (i.e. the 2 anode heel effect settings). Then, based on suitable image quality and lowest E, the optimised setting was identified.

### *Focal spot*

Focal spot was optimised using the same procedure as for anode heel effect. However, images were acquired at each: 1) broad (1.2mm); and 2) fine focus (0.6mm). Exposure time was recorded for all images, as this can be different between the 2 foci.

### *OID and air gap*

As both OID and air gap are indicators of the distance between the exposed object and the IR, air gap is implicitly optimised by optimising the OID. OID was optimised using the same procedure as for anode heel effect. However, images were acquired at each: 1) OID=0cm (in contact with the phantom); 2) OID=15cm; and 3) OID=30cm. The latter 2 OIDs were chosen as they have been reported appropriate for vertebral column imaging<sup>11, 12, 27</sup>.

Due to the different ways in which an OID can be created, OID was investigated twice:

1. Increasing the SID associated with the 64 combinations from step 1 by the 3 OIDs (0cm, 15cm and 30cm) (i.e. SOD [source to object distance] was fixed);
2. Decreasing the SOD by the 3 OIDs (0cm, 15cm and 30cm) (i.e. SID associated with the 64 combinations from step 1 was fixed).

### *Grid*

A reciprocating 10:1 focus grid (Wolverson, UK) was used, because it is common in clinical practice<sup>5</sup>. The use of a grid was optimised using a similar procedure to anode heel effect. However, images were acquired at each: 1) no grid (OID=0cm); and 2) grid. Also, the 64 combinations of kVp, mAs and SID were slightly modified in that the SID was fixed at 110cm to avoid grid cut-off as specified by the manufacturer.

### Step 3 – Conduct a full-factorial primary acquisition parameter investigation

For this, the primary acquisition parameters were investigated based on images acquired at all combinations of kVp, mAs and SID settings with the secondary acquisition parameters fixed at their optimised settings identified in step 2.

Images were acquired using 60 to 95kVp (stepping through 5kVp increments) in relation to 22 to 55mAs (stepping through 2mAs increments when applicable) in relation to 90 to 140cm SID (stepping through 5cm SID increments). The increments were based on preliminary work in which the minimum to trigger a change in image quality was identified. Also, the maximum and minimum primary acquisition parameter settings were chosen based on 2 settings above and 2 settings below the

highest and lowest kVp, mAs and SID settings from the 64 combinations established in step 1, respectively. The reason for doing this was to investigate whether combinations of primary acquisition parameters from ranges outside the established ranges from step 1 were associated with suitable image quality from lower E.

Acquired images were appraised with the VARS, and E was estimated for only the combinations of primary acquisition parameter settings associated with suitable image quality. These combinations were then ranked according to E values.

#### **4) Details of part 2 (human study)**

Knowing that there may be differences between phantoms and humans, the ranked combinations of acquisition parameters from part 1 (phantom study) were tested on humans.

### **Results and Discussion**

#### **Part 1 – Phantom study**

##### **Step 1 – Establish a factorial set of primary acquisition parameters**

The acquisition parameter combination that produced suitable image quality was 80kVp, 39mAs and 120cm SID. Based on these settings, the 64 combinations of primary acquisition parameters that were used during step 2 (again, which also involved 2 settings below and 1 above each obtained setting) were 70, 75, 80 and 85kVp in relation to 27, 33, 39 and 45mAs in relation to 100, 110, 120 and 130cm SID.

## Step 2 – Optimise each secondary acquisition parameter individually

### *Anode heel effect*

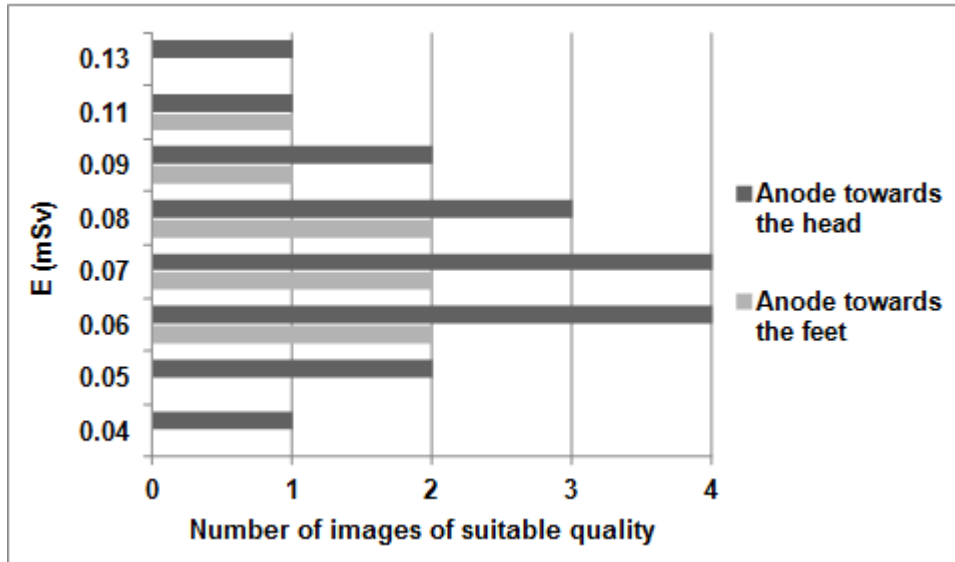


Figure 1. This gives the number of times each E produced a suitable image quality for the 2 anode heel effect settings (no zeros shown). 64 images were acquired at each setting, whereby the figure presents only images associated with suitable quality.

E to produce suitable image quality was either the same or lower when the anode was towards the head than towards the feet (Figure 1). This contradicts Fung & Gilboy<sup>28</sup>, who investigated dose absorbed by various organs in relation to both anode heel effect settings from a lateral lumbar spine exposure (28.81mGy entrance skin dose). With the anode towards the feet, they found an organ dose reduction of 385µGy and 3.7µGy for ovaries and testes, respectively. There was an increase of 3µGy, 0.4µGy, 0.1µGy for breasts, thyroids, and eye lenses, respectively. However, they used the same exposure factors of 96kVp and 120mAs for both anode heel effect settings, and did not consider optimising for image quality. This is perhaps why their findings differ from this study. Based on the above, 'anode towards the head' is the optimised setting.

### *Focal spot*

In agreement with others<sup>29</sup>, this study showed that E associated with suitable image quality was the same at both foci (Table 3). Also, acquisition time was always 47-80ms shorter with a broad focus. Reducing acquisition time would likely reduce patient movement and therefore motion blur. Based on the above, 'broad' is the optimised setting.

Table 3. The different Es are shown in ascending order, whereby the number of times each E produced a suitable image quality is shown for the 2 focal spot settings' exposure times (no zeros shown). 64 images were acquired at each setting, whereby the table presents only images associated with suitable quality.

Broad focus (ms)				E (mSv)	Fine focus (ms)				
63	71	90	100		110	125	140	160	180
1				0.04	1				
1	1			0.05		1	1		
2	1	1		0.06	2	1	1		
	2	2		0.07		2	2		
2			1	0.08	2				1
	1	1		0.09		1	1		
		1		0.11				1	
			1	0.13					1

### *OID or air gap*

Suitable image quality could be produced from lower E at OID=0cm than at OID=15 and 30cm (Table 4). Although in agreement with other studies<sup>5, 30</sup>, the findings from this study are in contradiction to Trout et al.<sup>27</sup>, who suggested that images of similar quality can be produced at 0 and 15cm OIDs from the same E by adjusting SID to a long setting. This contradiction might be because those authors considered image contrast, rather than a visual scale, as a tool for identifying suitable image

quality. Therefore, their conclusion is questionable, because they were not looking for diagnostic criteria in their image quality definition. Following OID investigation, the optimised OID setting is '0cm'.

Table 4. The different Es are shown in ascending order, whereby the number of times each E produced a suitable image quality is shown for the 3 OID settings (no zeros shown). 64 images were acquired at each setting, whereby the table presents only images associated with suitable quality.

OID (cm)		E (mSv)		OID (cm)	
0				15	30
1		0.04			
2		0.05			
5		0.06			
4		0.07			
5		0.08			
3		0.09			
		0.10		1	
1		0.11		1	
		0.12		1	
1		0.13			1
		0.14		1	2
		0.15			1
		0.16		2	2
		0.19		1	1
		0.20		1	
		0.23		2	
		0.27			1
		0.32			1
		0.36			2

## Grid

E to produce suitable image quality was always lower at OID=0cm than with a grid (Figure 2). In particular, the grid required an increase of at least 0.1mSv to produce the same image quality (i.e. the same VARS scores). Therefore, the optimised setting is 'OID=0cm'.

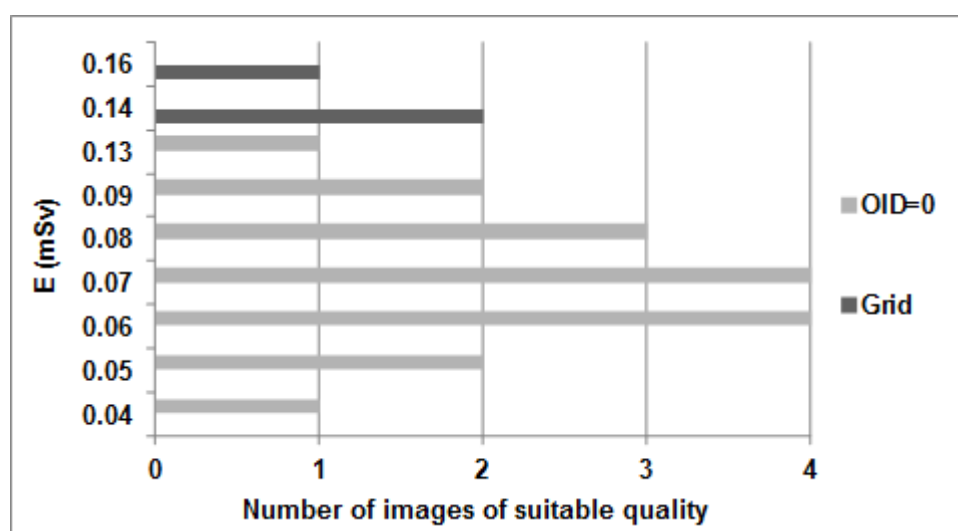


Figure 2. This gives the number of times each E produced a suitable image quality for OID=0cm and grid settings (no zeros shown). 64 images were acquired at each setting, whereby the figure presents only images associated with suitable quality.

### Step 3 – Conduct a full-factorial primary acquisition parameter investigation

From the 880 combinations of primary acquisition parameter of the full-factorial investigation (i.e. 8 kVp × 10mAs × 11 SID = 880), images of suitable quality were produced from only 74 of these combinations. The combinations mainly ranged from 75 to 90kVp, from 27 to 45mAs, and from 100 to 130cm SID (Figure 3).

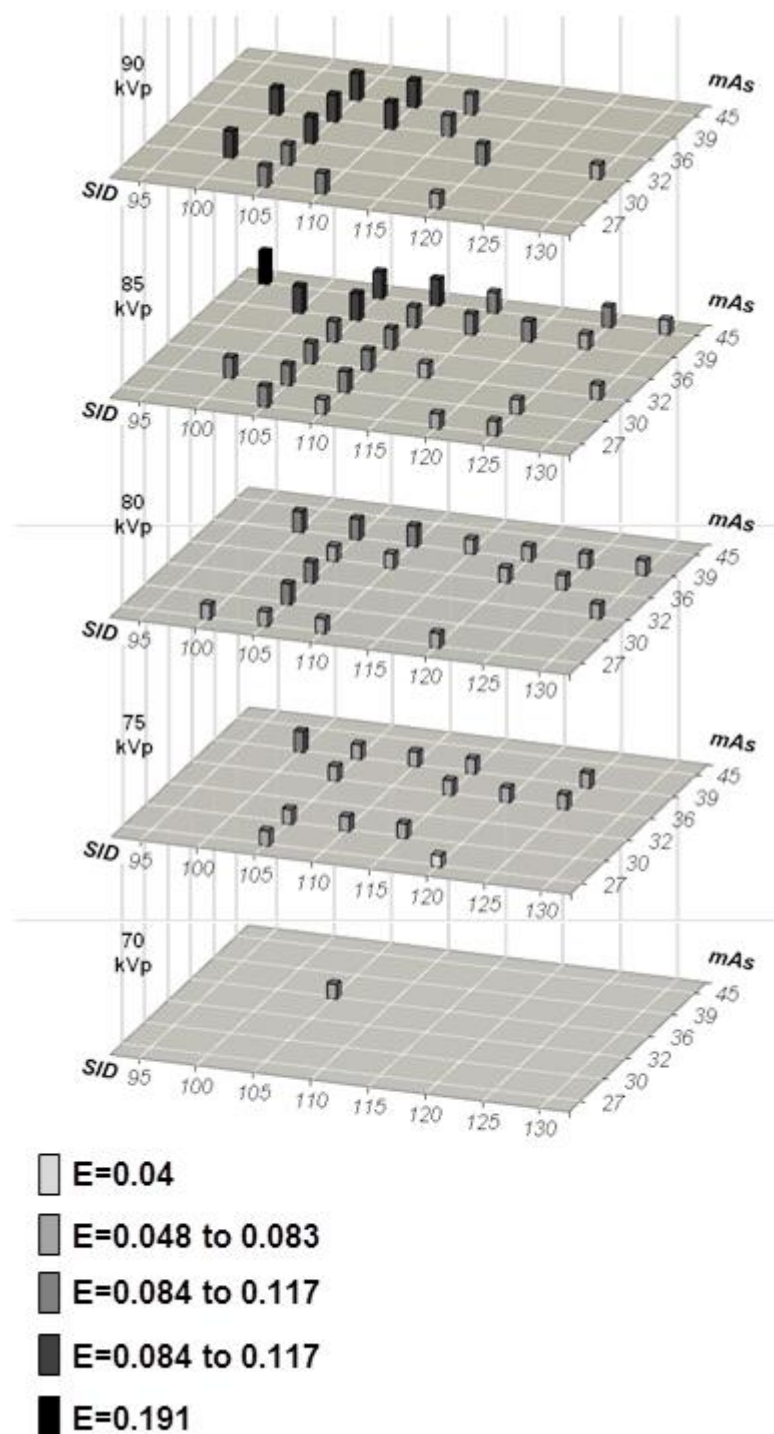


Figure 3. This gives the 74 combinations of kVp, mAs and SID settings that produced images of suitable quality with the anode towards the head, broad focus, OID=0cm (IR in contact with the volunteer), and no grid settings. Any column represents a combination of settings that produced a suitable image quality. For better illustration purposes, the increase in column height and darkness indicate an increase in E (measured in mSv).

Table 5 demonstrates a sample of the estimated E from the 74 combinations of primary acquisition parameter settings that produced the 74 images of suitable quality (whilst the secondary acquisition parameters were fixed at their optimised



settings).

Table 5. A sample of the 20 lowest Es is shown in conjunction with the associated primary acquisition parameter settings. The secondary acquisition parameters were fixed at their optimised settings: with the anode towards the head, broad focal spot size, and OID=0cm. The corresponding air Kerma is also listed.

<b>E</b>	<b>Air Kerma</b>	<b>Exposure factors</b>		
		<b>kVp</b>	<b>mAs</b>	<b>SID</b>
<b>0.040</b>	<b>1.25</b>	<b>75</b>	<b>27</b>	<b>120</b>
<b>0.048</b>	<b>1.45</b>	<b>75</b>	<b>36</b>	<b>125</b>
<b>0.049</b>	<b>1.48</b>	<b>80</b>	<b>27</b>	<b>120</b>
<b>0.050</b>	<b>1.50</b>	<b>80</b>	<b>32</b>	<b>130</b>
<b>0.052</b>	<b>1.58</b>	<b>75</b>	<b>30</b>	<b>115</b>
<b>0.053</b>	<b>1.63</b>	<b>75</b>	<b>36</b>	<b>120</b>
<b>0.053</b>	<b>1.61</b>	<b>75</b>	<b>40</b>	<b>125</b>
<b>0.054</b>	<b>1.46</b>	<b>85</b>	<b>27</b>	<b>125</b>
<b>0.056</b>	<b>1.83</b>	<b>75</b>	<b>30</b>	<b>110</b>
<b>0.057</b>	<b>1.86</b>	<b>75</b>	<b>27</b>	<b>105</b>
<b>0.059</b>	<b>1.65</b>	<b>80</b>	<b>40</b>	<b>130</b>
<b>0.060</b>	<b>2.07</b>	<b>70</b>	<b>36</b>	<b>105</b>
<b>0.060</b>	<b>1.84</b>	<b>75</b>	<b>36</b>	<b>115</b>
<b>0.060</b>	<b>1.67</b>	<b>80</b>	<b>36</b>	<b>125</b>
<b>0.060</b>	<b>1.65</b>	<b>85</b>	<b>27</b>	<b>120</b>
<b>0.060</b>	<b>1.64</b>	<b>85</b>	<b>30</b>	<b>125</b>
<b>0.062</b>	<b>1.88</b>	<b>80</b>	<b>27</b>	<b>110</b>
<b>0.064</b>	<b>2.09</b>	<b>75</b>	<b>30</b>	<b>105</b>
<b>0.065</b>	<b>2.05</b>	<b>75</b>	<b>39</b>	<b>115</b>
<b>0.066</b>	<b>1.88</b>	<b>80</b>	<b>36</b>	<b>120</b>

These 74 combinations of primary acquisition parameter settings, together with the optimised secondary acquisition parameters settings, formed a list of ranked

radiographic practices (based on E) for producing lateral T9 to L3 images from a reduced E.

The results show that images acquired at SIDs above 100cm but below 130cm may have the same image quality. Additionally, images acquired at SIDs less than 100cm had a considerably reduced quality in comparison to those acquired at SID above 130cm. Also, images acquired based on a range of SIDs from 100cm up to 130cm may have the same image quality. This was in contradiction to Brennan and Nash<sup>31</sup>, who found reduced sharpness of superior and inferior endplates with increasing SIDs from 100 to 130cm (whilst other acquisition parameters were fixed) in a lateral lumbar exposure. However, they suggested that this is due to grid cut-off, rather than increase in SID, which agrees with findings from the current study where a without grid exposure in conjunction with an SID of 100cm up to 130cm (whilst other acquisition parameters were fixed) reproduced the superior and inferior endplates clearly.

Further, with the same kVp and mAs settings, when SID increases above 100cm, the E steadily reduces, and the image quality is not affected until the SID exceeds 130cm. This is in agreement with other investigations that found a marked entrance surface dose and E reduction of approximately 12.5% and 45%, respectively (without affecting image quality) when SID increased above 100cm up to 130cm in lateral lumbar exposures<sup>32</sup>.

Furthermore and in accordance with other investigations<sup>33</sup>, a relatively low setting of both kVp and mAs was associated with suitable image quality in this study. This was the case possibly because images are considered suitable as long as they can be used for Cobb and superimposition method measurements, regardless of image

noise.

## Part 2 – Human study

The combination of acquisition parameter settings from the phantom-based study associated with the 4<sup>th</sup> lowest ranked E (rather than the 1<sup>st</sup> lowest ranked E) was the one that produced human volunteer images of suitable quality from the lowest E (Figure 4). This optimised combination was successful in producing images of suitable quality from human volunteers whilst standing upright and with the trunk flexed and extended.



Figure 4. This gives a lateral thoraco-lumbar exposure of one of the human living volunteers using the identified optimised combination of acquisition parameter settings (i.e. 80kVp, 32mAs, 130cm SID, anode towards the head, broad focus, OID=0cm (IR in contact with the volunteer ), and with no grid).

At the hospital where the human study took place, lateral thoraco-lumbar spine X-ray imaging for Cobb method measurements is typically associated with an E of 1mSv from using 90kVp, 100mAs, 100cm SID, no concern for anode heel effect, broad

focus, and a grid (and hence no concerns for the OID). In contrast, as identified in the human study, the combination of acquisition parameter settings associated with suitable image quality from an E of 0.05mSv were 80kVp, 32mAs, 130cm SID, anode towards the head, broad focus, OID=0cm (IR in contact with volunteer), and no grid. This E of 0.05mSv represents a reduction of almost 95% from that used in the hospital, and 83% from the average E used in the UK (0.3mSv) for lateral thoracic or lumbar imaging<sup>34</sup>.

The current investigation was novel in that the complex effect of multiple acquisition parameters (at their available settings) on image quality and dose was investigated and resulted in a new X-ray practice that was tested successfully on living human volunteers. In addition, obtained results could reduce risks of exposures on a large population of spinal deformation patients whose assessment is based on Cobb or superimposition method measurements. More importantly, although being focused on Cobb and superimposition measurements, this paper presents a newly developed and successful procedure for optimising different X-ray practices based on reducing dose without affecting diagnostic image quality.

Nevertheless, further investigations in this area of research are needed. In particular, parameters other than the ones investigated in the current paper as, for example, other grid types need to be considered. Also, optimisation for people with different sizes (not only normal-weight) should be considered. Additionally, although the results from the study were tested on 9 healthy volunteers, studies on larger sample sizes are needed to make generalisation of obtained practice possible. Finally, in the current investigation and due to time restrictions and the huge number of tested parameters, dose was estimated from air Kerma; whereby dose estimated from TLD

readings could be more precise.

## **Conclusion**

This study was based on a new systematic optimisation procedure to identify the settings of the main acquisition parameters that would produce a suitable lateral thoraco-lumbar spine X-ray image for inter-vertebral angulation measurements using Cobb and superimposition methods from the lowest E. The obtained acquisition parameter settings and resultant optimised radiographic practice was then validated by imaging healthy normal-weight male adult living human volunteers. The specific optimised radiographic practice that emerged from this procedure produced suitable image quality from ALARP E using anode towards the head, broad focus, no OID or grid, 80kVp, 32mAs, 130cm SID. With an E of 0.05mSv, this is approximately 83% less than the average E of 0.3mSv used in the UK<sup>30</sup> for lateral thoracic or lumbar imaging. The new optimisation procedure was successful in identifying suitable image quality whilst greatly reducing E. Although this procedure was developed for lateral thoraco-lumbar spine exposures, it might also be adopted for the optimisation of other radiographic procedures.

## **References:**

- [1] A. De Smet, S. Fritz, M. Asher, A method for minimizing the radiation exposure from scoliosis radiographs. *The Journal of Bone and Joint Surgery* 63 (1981), 156-61.
- [2] ICRP. Recommendations of the international Commission on Radiological Protection, Publication 26, Oxford, Pergamon Press. ICRP 1977.
- [3] NRPB. National Radiological Protection Board. dose reduction in diagnostic

- radiology. London: HMSO, Documents of the NRPB. 1990; 1(3).
- [4] R. Berry, Striking a balance: benefit and risk in man's exposure to man-made radiations. *British Journal of Radiology* 65 (1992), 1-8.
  - [5] T. Fauber, *Radiographic imaging and exposure*. 3 ed. Missouri, USA: Mosby Inc., 2009.
  - [6] G. Hellström, L. Irstam, A. Nachemson, Reduction of radiation dose in radiologic examination of patients with scoliosis. *Spine* 8(1983), 28-30.
  - [7] J. Cobb, Outline for the study of scoliosis: instructional course lectures, the American Academy of Orthopaedic Surgeons. 1948.
  - [8] A. Begg and M. Falconer, Plain radiography in intraspinal protrusion of lumbar intervertebral disks; a correlation with operative findings. *The British Journal of Surgery* 36(1949), 220:225.
  - [9] G. Ardran, R. Coates, R. Dickson, Assessment of scoliosis in children: low dose radiographic technique. *British Journal of Radiology* 53(1980), 140-146.
  - [10] S. Hallen, K. Martling, S. Mattsson, Dosimetry at x ray examinations of scoliosis. *Radiation Protection Dosimetry* 43(1992), 49-54.
  - [11] J. Hansen, A. Jurik, B. Fiirgaard, Optimisation of scoliosis examinations in children. *Pediatric Radiology* 33(2003), 752-65.
  - [12] A. Jónsson, K. Jonsson, K. Eklund, Computed radiography in scoliosis. Diagnostic information and radiation dose. *Acta Radiologica* 36(1995), 429-33.
  - [13] M. Kogutt, F. Warren, J. Kalmar, Low dose imaging of scoliosis: use of a

- computed radiographic imaging system. *Pediatric Radiology* 20(1989), 85-86.
- [14] J. Lescreve, R. Tiggelen, J. Lamoureux, Reducing the radiation dosage in patients with a scoliosis. *International Orthopaedics* 13(1989), 47-50.
- [15] A. Kalmar, P. Jones, R. Christopher, Low-Dose Radiography of Scoliosis in Children: A Comparison of Methods. *Spine* 19(1994), 48-54
- [16] C. Nash, E. Gregg, R. Brown, K. Pillai, Risks of exposure to X-rays in patients undergoing long-term treatment for scoliosis. *J Bone Joint Surg Am* 61(1979), 371-374
- [17] J. Hsu, J. Michael, J. Fisk, editors. *AAOS atlas of orthoses and assistive devices*. 4 ed. Philadelphia, USA: Mosby Inc., 2008.
- [18] A. Servomaa and M. Tapiovaara, Organ dose calculation in medical x ray examinations by the program PCXMC. *Radiation Protection Dosimetry* 80(1998), 213-19.
- [19] Commission of the European communities: European guidelines on quality criteria for diagnostic radiographic images. EUR 1620 EN, CEC, Brussels 1996.
- [20] A. Viera and J. Garrett, Understanding interobserver agreement: the kappa statistic. *Family Medicine* 37(2005), 360-3.
- [21] F. Joseph, Measuring nominal scale agreement among many raters. *Psychological Bulletin* 76(1971), 378-382
- [22] P. Andreo, Monte Carlo techniques in medical radiation physics. *Physics in Medicine and Biology* 36(1991), 861-920.

- [23] D. Jones and B. Wall, Organ doses from medical x-ray examinations calculated using Monte Carlo techniques. NRPB Publication NRPB-R186 (National Radiological Protection Board, Chilton, Oxon) 1985.
- [24] ICRP. The 2007 Recommendations of the International Commission on Radiological Protection. ICRP Publication 103. Ann. ICRP 37 (2-4). 2007.
- [25] A. Whitley, *Clark's positioning in radiography*. London, UK: Hodder Arnold, 2005.
- [26] P. Hiles, A. Mackenzie, A. Scally, *Recommended standards for the routine performance testing of diagnostic X-ray imaging systems*. Institute of Physics and Engineering in Medicine 2005;Report No 91.
- [27] E. Trout, J. Kelley, V. Larson, A comparison of an air gap and a grid in roentgenography of the chest. *American Journal of Roentgenology* 124(1975), 404-11.
- [28] K. Fung and W. Gilboy, "Anode heel effect" on patient dose in lumbar spine radiography. *British Journal of Radiology* 73(2000), 531-36.
- [29] S. Gorham and P. Brennan, The impact of focal spot size on clinical images (Proceedings Paper). 2009.
- [30] T. Curry, J. Dowdey, R. Murry, Christensen's physics of diagnostic radiology. Philadelphia, USA: Lippincott Williams & Wilkins, 1990.
- [31] P. Brennan and M. Nash, Increasing FFD: an effective dose-reducing tool for lateral lumbar spine investigations. *Radiography* 4(1998), 251-59.



- [32] P. Brennan, S. McDonnell, D. O'Leary, Increasing film-focus distance (ffd) reduces radiation dose for x-ray examinations. *Radiation Protection Dosimetry* 108(2004), 263-68.
- [33] S. Etemadinezhad, S. Rahimi, Patient exposure dose for chest and skull radiographies in Mazandaran hospitals. *Rahimi, Xray Sci Technol.* 18(2010), 87-91.
- [34] B. Wall and D. Hart, Revised radiation doses for typical X-ray examinations. Report on a recent review of doses to patients from medical X-ray examinations in the UK by NRPB. National Radiological Protection Board. *British Journal of Radiology* 70(1997), 437-39.
- [35] J. Landis and G. Koch The measurement of observer agreement for categorical data. *Biometrics* 33(1977), 159-174.